

# Precise Sm–Nd and U–Pb isotopic dating of the supergiant Shizhuyuan polymetallic deposit and its host granite, SE China

XIAN-HUA LI\*†§, DUNYI LIU‡, MIN SUN†, WU-XIAN LI\*,  
XI-RONG LIANG\* & YING LIU\*

\*Guangzhou Institute of Geochemistry, Chinese Academy of Sciences, P.O. Box 1131, Guangzhou 510640, China

†Department of Earth Sciences, The University of Hong Kong, Pokfulam Road, Hong Kong, China

‡Beijing SHRIMP Centre, Institute of Geology, Chinese Academy of Geological Sciences, Beijing 10037, China

(Received 13 February 2003; accepted 4 November 2003)

**Abstract** – The supergiant Shizhuyuan W–Sn–Bi–Mo deposit is hosted by the Qianlishan granite, a small, highly fractionated granitic pluton ( $\sim 10 \text{ km}^2$ ) with multiple phases of intrusions within the Early Yanshanian granitoid province of SE China. Strong alteration of skarn and greisen that formed in the contact zone between the first and second phases of granite intrusions and Devonian limestone is responsible for the polymetallic mineralizations. SHRIMP U–Pb zircon analysis indicates that the two early phases of the Qianlishan granite formed contemporaneously at  $152 \pm 2 \text{ Ma}$ . Metasomatic minerals (garnet, fluorite and wolframite) separated from the skarn and greisen yield a Sm–Nd isochron age of  $149 \pm 2 \text{ Ma}$  that is interpreted as the formation age of the Shizhuyuan deposit. Therefore, the mineralization of the supergiant Shizhuyuan polymetallic deposit formed contemporaneously with, or very shortly after, the intrusion of the small, highly fractionated Qianlishan granite.

Keywords: Sm–Nd, U–Pb, geochronology, granite, South China Block.

## 1. Introduction

The Mesozoic geology of SE China is characterized by intensive and widespread granitic plutonism associated with numerous non-ferrous and rare metal mineral deposits (Pei & Hong, 1995). Among these ore deposits, the Shizhuyuan polymetallic deposit is one of the largest non-ferrous metal deposits in the world, containing 80 Mt W, 40 Mt Sn, 20 Mt Bi and 10 Mt Mo as well as substantial amounts of Be, Pb, Zn, Ag, F and B (Wang *et al.* 1987; Mao *et al.* 1998). Thus, it is a high-grade supergiant polymetallic deposit in the classification terms of Laznicka (1999). This polymetallic deposit has long been suggested to be genetically related in time and space to the Qianlishan granitic pluton, with strong skarn and greisen alteration being responsible for the W–Sn–Mo–Bi mineralization (Liu, Zhang & Chen, 1983; Wang *et al.* 1987; Mao *et al.* 1995, 1998). While many geochronological investigations have been carried out on the Qianlishan granite and the Shizhuyuan deposit since the mid-1980s, the previously published radiometric dates either span a wide time interval, or are inconsistent with each other. Therefore, the timing of granitic plutonism and polymetallic mineralization remains controversial. In this paper we present high-precision SHRIMP U–Pb zircon and Sm–Nd mineral isochron ages for the Qianlishan granite and the mineralization at Shizhuyuan. These new results provide a rigorous constraint

on the timing of granitic plutonism and its temporal relationship to the polymetallic mineralization.

## 2. Geological background

The Qianlishan granite pluton crops out over  $\sim 10 \text{ km}^2$ , about 15 km southeast of Chengzhou City (Hunan Province), and is located within the Early Yanshanian (mainly Jurassic) granitoid province of South China (Fig. 1). It intrudes into Devonian sandstone and limestone. Based on field relationships, the granite pluton consists of multiple phases of magmatic intrusion (Wang *et al.* 1987). The first phase ( $\gamma_5^{2a}$ ) is a porphyritic biotite granite with an outcrop area of  $1.2 \text{ km}^2$  occurring in the southern part of the pluton. Phenocrysts of quartz range in size from 1 to 3 cm. The second phase ( $\gamma_5^{2b}$ ) is an equigranular biotite granite with a total outcrop area of  $8.4 \text{ km}^2$ . This forms the main body of the Qianlishan granite and consists of an inner phase of medium- to coarse-grained biotite granite and a marginal phase of fine- to medium-grained biotite granite. The third phase ( $\gamma_5^{2c}$ ) comprises small fine-grained porphyritic biotite granitic stocks (total area =  $0.2 \text{ km}^2$ ) that intruded into the earlier two phases of granite. The fourth phase ( $\gamma_5^{2d}$ ) comprises a NE-striking dyke swarm of granite porphyry and quartz porphyry. All these granitic rocks were cut by mafic dykes of mainly N–S orientation (Wang *et al.* 1987).

The Shizhuyuan polymetallic deposit is of the skarn-greisen type formed in the contact zone between the

§ Author for correspondence: lixh@gig.ac.cn

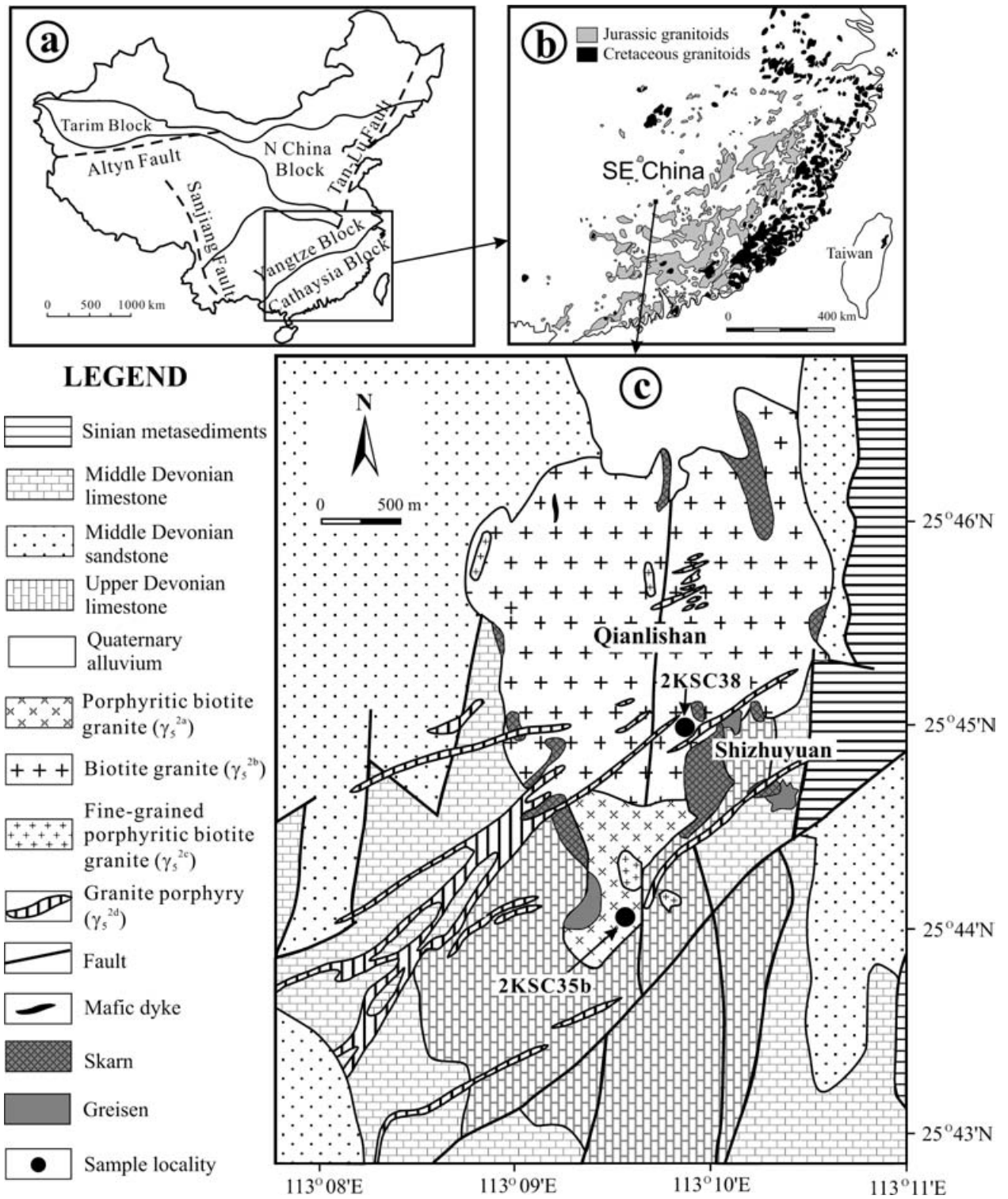


Figure 1. (a) Simplified map showing the main plate-scale tectonic units of China. (b) Distribution of Yanshanian granitoids in SE China, with the Early Yanshanian (mainly Jurassic) granitoid province within the interior and the Late Yanshanian (mainly Cretaceous) granitoid province along the coastal region (after Li, 2000). (c) Geological map of the study area illustrating the Qianlishan granite and the Shizhuyuan deposit (after Wang *et al.* 1987).

Qianlishan granite and Devonian limestone country rocks. Field relations indicate that the deposit is closely related in time and space to the first and second phases of granitic intrusion (Wang *et al.* 1987). Two stages of metasomatic mineralization are

identified by Mao *et al.* (1996): (1) an early stage of massive-type skarn-greisen W–Sn–Mo–Bi mineralization associated with porphyritic biotite granite ( $\gamma_s^{2a}$ ), and (2) a late stage of vein-type greisen W–Sn–Mo–Bi–Be–Pb–Zn–Ag mineralization

associated with medium- to coarse-grained biotite granite ( $\gamma_5^{2b}$ ).

### 3. Previous radiometric dates

Numerous chronological investigations on the Qianlishan granitic rocks and Shizhuyuan deposit have been carried out, and the results are summarized below.

*Porphyritic biotite granite ( $\gamma_5^{2a}$ ).* Wang *et al.* (1987) first reported a Rb–Sr isochron date of  $182 \pm 9$  Ma, which is identical within analytical errors to a K-feldspar  $^{40}\text{Ar}$ – $^{39}\text{Ar}$  plateau date of  $183 \pm 4$  Ma reported by Liu *et al.* (1997). In contrast, Mao, Li & Pei (1995) obtained a younger Rb–Sr isochron date of  $152 \pm 9$  Ma. Muscovite and biotite from the porphyritic biotite granite yielded K–Ar dates of  $142.6 \pm 2.8$  Ma and  $144.5 \pm 3.4$  Ma (Yin *et al.* 2002), respectively, which were interpreted as greisen alteration overprinting related to the W–Sn–Mo–Bi mineralization.

*Fine- and medium-grained biotite granite ( $\gamma_5^{2b}$ ).* Radiometric dates reported for the medium-grained biotite granite span a wide range from  $163 \pm 3$  Ma for a K-feldspar  $^{40}\text{Ar}$ – $^{39}\text{Ar}$  plateau date (Liu *et al.* 1997),  $149.3 \pm 3.5$  Ma for a muscovite K–Ar date (Yin *et al.* 2002), to  $146 \pm 1$  Ma for a Rb–Sr isochron date (Shen *et al.* 1995). In addition, Mao, Li & Pei (1995) obtained Rb–Sr isochron dates of  $137 \pm 7$  Ma and  $136 \pm 6$  Ma for the medium- and fine-grained biotite granites, respectively.

*Fine-grained porphyritic biotite granite ( $\gamma_5^{2c}$ ).* A muscovite K–Ar date of  $137.4 \pm 3.3$  Ma was reported by Yin *et al.* (2002).

*Granite porphyry ( $\gamma_5^{2d}$ ).* Mao, Li & Pei (1995) reported a Rb–Sr isochron date of  $131 \pm 1$  Ma for the granite porphyry. However, this Rb–Sr date is significantly younger than the K-feldspar  $^{40}\text{Ar}$ – $^{39}\text{Ar}$  plateau date of  $144 \pm 3$  Ma obtained from another porphyry dyke (Liu *et al.* 1997).

*Polymetallic mineralization.* Li *et al.* (1996) reported a Re–Os isochron date of  $151 \pm 4$  Ma for molybdenite from the early stage of mineralization. Later, a Sm–Nd isochron date of  $161 \pm 2$  Ma (recalculated as  $161 \pm 19$  Ma using Isoplot/Ex 2.49 of Ludwig, 2001) was obtained from five garnet samples and one diopside sample from the skarn (Liu *et al.* 1997). More recently, Yin *et al.* (2002) reported muscovite K–Ar dates of  $146.5 \pm 2.9$  Ma and  $148.0 \pm 2.9$  Ma for the early massive-type greisen and the late vein-type greisen, respectively.

In general, the aforementioned radiometric dates suggest a time interval of Middle Jurassic to earliest Cretaceous for the main phases of the Qianlishan granite ( $\gamma_5^{2a}$  and  $\gamma_5^{2b}$ ) and a mainly Late Jurassic time for the polymetallic deposit at Shizhuyuan, whereas the precise ages of the granite and the deposit remain controversial. Hence, the temporal relationships

between the plutonism and polymetallic mineralization are still poorly constrained.

### 4. Analytical methods

The mineral fractions for isotopic analyses in this study were processed using conventional magnetic and density techniques. Final mineral separates of the best-quality grains were extracted from each concentrate by hand-picking under a binocular microscope.

For the U–Pb analysis, zircon grains, together with a zircon U–Pb standard, were cast in an epoxy mount, which was then polished to section the crystals in half for analysis. Zircons were documented with transmitted and reflected light micrographs and back-scattered electron (BSE) images, and the mount was vacuum-coated with a 500 nm layer of high-purity gold. Measurements of U, Th and Pb were conducted using a SHRIMP II ion microprobe newly installed in the Institute of Geology, Chinese Academy of Geological Sciences, Beijing. U–Th–Pb ratios were determined relative to the TEMORA standard zircon ( $^{206}\text{Pb}/^{238}\text{U} = 0.0668$  corresponding to 417 Ma: Black *et al.* 2003a,b), and the absolute abundances were calibrated to the SL13 standard zircon ( $^{238}\text{U} = 238$  ppm). Analyses of the TEMORA standard zircon were interspersed with those of unknown grains, following operating and data processing procedures similar to those described by Williams (1998) and Song *et al.* (2002). The mass resolution used to measure Pb/Pb and Pb/U isotopic ratios was about 5000 during the analyses. Measured compositions were corrected for common Pb using  $^{208}\text{Pb}$  methods by assuming  $^{206}\text{Pb}/^{238}\text{U}$ – $^{208}\text{Pb}/^{232}\text{Th}$  age-concordance. Corrections are sufficiently small to be insensitive to the choice of common Pb composition, and an average crustal composition (Cumming & Richards, 1975) appropriate to the age of the mineral was assumed. Uncertainties on individual analyses are reported at the  $1\sigma$  level; mean ages for pooled  $^{206}\text{Pb}/^{238}\text{U}$  results are quoted at 95 % confidence level.

For the Sm–Nd investigations, garnet, fluorite and wolframite were rinsed repeatedly with 1N HCl and ultra-pure water in an ultrasonic bath, and then ground to 200 mesh using an ultra-clean agate mortar. These sample powders were then subjected to step-wise leaching procedures modified after Blichert-Toft & Frei (2001) and Thöni (2002). The garnet was leached by means of 6N HCl, 11.4N HCl and a mixture of 2:1 7N  $\text{HNO}_3$ /6N HCl. Each leaching step was performed in an ultrasonic bath for 20 minutes followed by 1 hour on a hot plate at  $100^\circ\text{C}$ . The garnet sample was rinsed three times with ultra-pure water, and separation of the residue from the leaching solution was performed by centrifuging. The fluorite and wolframite were leached ultrasonically by means of 2N HCl, 5 % HF and 2N HCl for 20 minutes, and then rinsed three times with ultra-pure water. Chemical dissolution of garnet and fluorite was performed in high-pressure Teflon

bombs using a HF/HClO<sub>4</sub> mixture of 5:1 at  $T = 150^\circ\text{C}$  for 3 days. Wolframite was dissolved in concentrated HCl for 24 hours. All the sample dissolutions were split into two aliquots (IC and ID). Sm and Nd fractions were separated by passing through cation columns followed by HDEHP columns. Nd isotopic compositions (IC, unspiked aliquot) were determined using a Micromass Isoprobe multi-collector (MC-ICPMS) at the Guangzhou Institute of Geochemistry. Samples were taken up in 2 % HNO<sub>3</sub>, and the aqueous solutions were introduced into the MC-ICPMS using a Meinhard glass nebulizer in free-aspiration mode with an uptake rate of 0.1 mL/min. Nd concentrations in solutions were *c.* 200 ppb, and these yielded a <sup>144</sup>Nd ion beam of *c.*  $4 \times 10^{-11}$  A. An internal precision of less than 20 ppm on the <sup>143</sup>Nd/<sup>144</sup>Nd ratios was obtained for the Nd standards after 40 to 50 integrations. This corresponds to a usage of about 40–50 ng Nd. For analysis of the unknown samples, the same precision was obtained after 60 to 80 integrations corresponding to a usage of about 60–80 ng Nd. The inlet system was washed out for 5 minutes between analyses using high-purity 5 % HNO<sub>3</sub> followed by a blank solution of 2 % HNO<sub>3</sub> from which the sample solutions were prepared. The mass spectrometer was used in static multi-collector mode for this study. During the daily analytical session, we ran a laboratory standard (Nd-GIG) first, and then the Shin Etsu JNdi-1 standard once for every four unknown samples. The hydride interference was undetectable through elimination by the hexapole. The Isoprobe MC-ICPMS yielded <sup>143</sup>Nd/<sup>144</sup>Nd =  $0.512120 \pm 8$  ( $2\sigma_m$ ) and  $0.511530 \pm 7$  ( $2\sigma_m$ ) for the Shin Etsu JNdi-1 standard and the laboratory Nd-GIG standard, respectively, during the course of this study. A long-term (over five months) average of <sup>143</sup>Nd/<sup>144</sup>Nd is  $0.512120 \pm 12$  ( $2\sigma$ ) for the Shin Etsu JNdi-1 standard and  $0.511532 \pm 13$  ( $2\sigma$ ) for the Nd-GIG standard during the period of this study (Liang *et al.* 2003). Detailed analytical procedures are given by Liang *et al.* (2003) modified after Vance & Thirlwall (2002). Measured <sup>143</sup>Nd/<sup>144</sup>Nd ratios were normalized to <sup>146</sup>Nd/<sup>144</sup>Nd = 0.7219. Sm and Nd concentrations (ID, spiked with a mixed <sup>146</sup>Nd–<sup>149</sup>Sm tracer) were measured on a VG-354 mass spectrometer operated in dynamic multi-collector mode at the Guangzhou Institute of Geochemistry. The in-run error of Sm and Nd is generally  $\leq 0.1\%$ , whereas the external error based on duplicate analyses of rock powders is estimated at  $\sim 0.5\%$ . The reported <sup>143</sup>Nd/<sup>144</sup>Nd ratios are adjusted relative to the Shin Etsu JNdi-1 standard of 0.512115, corresponding to the La Jolla standard of 0.511860 (Tanaka *et al.* 2000).

## 5. Results

### 5.a. U–Pb zircon ages of the Qianlishan granite

Sample 2KSC35b, a porphyritic biotite granite ( $\gamma_5^{2a}$ ), was collected from the southern part of the pluton

( $25^\circ44.046' \text{N}$ ,  $113^\circ09.668' \text{E}$ ). Zircons in this sample are mostly euhedral, range up to 150–200  $\mu\text{m}$  in length, and have length to width ratios up to 3:1. Most crystals are transparent, colourless to slightly brown. Euhedral concentric zoning is common in most crystals. Inherited zircon cores can be occasionally observed, but they were not involved in the analyses in terms of the BSE images. Eighteen analyses of 18 magmatic zircons from sample 2KSC35b were obtained in sets of five scans during a single analytical session (Table 1). Uranium concentration is highly variable, ranging from 173 to 1100 ppm. Thorium ranges from 138 to 496 ppm, and Th/U ratios vary between 0.27 and 1.15. The U–Pb isotopic results form a single, concordant group with a weighted mean <sup>206</sup>Pb/<sup>238</sup>U age of  $153 \pm 3$  Ma (MSWD = 0.29). This age is interpreted as the crystallization age of sample 2KSC35b.

Sample 2KSC38, a medium-grained biotite granite ( $\gamma_5^{2b}$ ), was collected from the southeastern part of the pluton ( $25^\circ45.088' \text{N}$ ,  $113^\circ09.942' \text{E}$ ) (Fig. 1). Zircon crystals are very similar in shape and colour to those of sample 2KSC35b. Thirteen analyses of 13 magmatic zircons were obtained (Table 1). Uranium concentration ranges from 192 to 1678 ppm, and thorium from 67 to 723 ppm. Th/U ratios are relatively constant between 0.31 and 0.58. The <sup>206</sup>Pb/<sup>238</sup>U ratios for the 13 analyses agree to within analytical error, yielding a weighted mean age of  $151 \pm 3$  Ma (MSWD = 0.48). This age is interpreted as the crystallization age of sample 2KSC38.

The <sup>206</sup>Pb/<sup>238</sup>U ages of the above two samples are indistinguishable within analytical errors (Table 1, Fig. 2), indicating that the first and second phases of Qianlishan granite are contemporaneous. They are also co-genetic in terms of their geochemical and isotopic features (see Section 6). All 31 measured <sup>206</sup>Pb/<sup>238</sup>U ratios for the two samples can form a single, concordant population yielding a weighted mean age of  $152 \pm 2$  Ma (MSWD = 0.39), which is the best estimate of the crystallization age of the Qianlishan pluton ( $\gamma_5^{2a}$  and  $\gamma_5^{2b}$ ).

### 5.b. Sm–Nd isochron age of the Shizhuyuan polymetallic deposit

Metasomatic minerals separated from the skarn and greisen at the Shizhuyuan deposit are used for Sm–Nd isotopic analysis. These minerals include two garnet fractions and two fluorite fractions from the massive-type skarn, two wolframite fractions from the massive-type greisen, and one fluorite fraction from the vein-type greisen. The Sm–Nd isotopic data are listed in Table 2. Garnets have highly variable Sm (3.0–6.3 ppm) and Nd (2.3–11.8 ppm) contents and a wide range of <sup>147</sup>Sm/<sup>144</sup>Nd ratio (0.3214–0.7838). Fluorites from the massive-type skarn are generally high in Sm (7.6–15.9 ppm) and Nd (16.2–22.5 ppm)

Table 1. SHRIMP U–Pb zircon data for the Qianlishan granite

| Grain   | U (ppm) | Th (ppm) | Th/U | $f_{206}$ (%) | $^{207}\text{Pb}^*/^{235}\text{U}^*$ ( $\pm 1\sigma$ ) | $^{206}\text{Pb}^*/^{238}\text{U}$ ( $\pm 1\sigma$ ) | 206/238 age (Ma) ( $\pm 1\sigma$ ) |
|---|---------|----------|------|---------------|--|--|------------------------------------|
| 2KSC35b ( $\gamma_5^{2a}$ ) (25°44.046' N, 113°09.668' E) |         |          |      |               |  |  |                                    |
| 1.1   | 579     | 232      | 0.41 | 1.35          | 0.153 $\pm$ 0.006                                      | 0.0235 $\pm$ 0.0008                                  | 149.7 $\pm$ 5.5                    |
| 2.1   | 223     | 167      | 0.77 | 1.40          | 0.146 $\pm$ 0.007                                      | 0.0242 $\pm$ 0.0009                                  | 154.0 $\pm$ 6.3                    |
| 3.1   | 1100    | 283      | 0.27 | 1.69          | 0.169 $\pm$ 0.006                                      | 0.0252 $\pm$ 0.0009                                  | 160.2 $\pm$ 5.7                    |
| 4.1   | 669     | 371      | 0.57 | 0.23          | 0.142 $\pm$ 0.006                                      | 0.0239 $\pm$ 0.0008                                  | 152.1 $\pm$ 5.8                    |
| 5.1   | 208     | 194      | 0.97 | 1.60          | 0.133 $\pm$ 0.008                                      | 0.0240 $\pm$ 0.0009                                  | 152.6 $\pm$ 6.5                    |
| 6.1   | 571     | 272      | 0.49 | 1.09          | 0.150 $\pm$ 0.006                                      | 0.0235 $\pm$ 0.0008                                  | 149.6 $\pm$ 5.6                    |
| 7.1   | 521     | 214      | 0.42 | 0.98          | 0.174 $\pm$ 0.007                                      | 0.0239 $\pm$ 0.0008                                  | 152.3 $\pm$ 5.6                    |
| S1.1  | 627     | 264      | 0.44 | 0.32          | 0.164 $\pm$ 0.006                                      | 0.0238 $\pm$ 0.0008                                  | 151.6 $\pm$ 5.6                    |
| S1.2  | 717     | 260      | 0.37 | 0.26          | 0.156 $\pm$ 0.006                                      | 0.0237 $\pm$ 0.0008                                  | 151.1 $\pm$ 5.6                    |
| S1.3  | 217     | 243      | 1.15 | 1.20          | 0.151 $\pm$ 0.008                                      | 0.0253 $\pm$ 0.0009                                  | 160.8 $\pm$ 7.1                    |
| S1.4  | 862     | 496      | 0.60 | 0.39          | 0.158 $\pm$ 0.006                                      | 0.0237 $\pm$ 0.0009                                  | 151.3 $\pm$ 5.9                    |
| S1.5  | 173     | 151      | 0.90 | 0.71          | 0.165 $\pm$ 0.008                                      | 0.0243 $\pm$ 0.0009                                  | 154.7 $\pm$ 6.4                    |
| S1.6  | 251     | 219      | 0.90 | 0.00          | 0.146 $\pm$ 0.007                                      | 0.0240 $\pm$ 0.0008                                  | 152.8 $\pm$ 6.3                    |
| S1.7  | 794     | 476      | 0.62 | 0.17          | 0.165 $\pm$ 0.006                                      | 0.0243 $\pm$ 0.0008                                  | 154.6 $\pm$ 5.9                    |
| S1.8  | 671     | 281      | 0.43 | 0.20          | 0.150 $\pm$ 0.006                                      | 0.0232 $\pm$ 0.0008                                  | 148.1 $\pm$ 5.5                    |
| S1.9  | 331     | 183      | 0.57 | 0.87          | 0.145 $\pm$ 0.009                                      | 0.0239 $\pm$ 0.0008                                  | 152.3 $\pm$ 5.9                    |
| S1.10   | 508     | 250      | 0.51 | 0.02          | 0.150 $\pm$ 0.006                                      | 0.0239 $\pm$ 0.0008                                  | 152.3 $\pm$ 5.8                    |
| S1.11   | 227     | 138      | 0.63 | 0.76          | 0.161 $\pm$ 0.007                                      | 0.0238 $\pm$ 0.0008                                  | 151.7 $\pm$ 6.0                    |
| Weighted mean ( $2\sigma$ )                               |         |          |      |               |  |  |                                    |
| 2KSC38 ( $\gamma_5^{2b}$ ) (25°45.088' N, 113°09.942' E)  |         |          |      |               |  |  |                                    |
| 1.1   | 221     | 67       | 0.31 | 5.04          | 0.170 $\pm$ 0.011                                      | 0.0238 $\pm$ 0.0008                                  | 151.6 $\pm$ 5.6                    |
| 2.1   | 383     | 138      | 0.37 | 0.62          | 0.162 $\pm$ 0.007                                      | 0.0239 $\pm$ 0.0008                                  | 152.3 $\pm$ 5.6                    |
| 3.1   | 204     | 83       | 0.42 | 2.94          | 0.145 $\pm$ 0.010                                      | 0.0233 $\pm$ 0.0008                                  | 148.4 $\pm$ 5.8                    |
| 4.1   | 294     | 116      | 0.41 | 6.41          | 0.152 $\pm$ 0.033                                      | 0.0240 $\pm$ 0.0008                                  | 153.0 $\pm$ 6.4                    |
| 5.1   | 242     | 104      | 0.45 | 5.23          | 0.150 $\pm$ 0.017                                      | 0.0243 $\pm$ 0.0009                                  | 154.8 $\pm$ 6.3                    |
| 6.1   | 476     | 199      | 0.43 | 1.26          | 0.162 $\pm$ 0.007                                      | 0.0248 $\pm$ 0.0009                                  | 158.1 $\pm$ 5.8                    |
| 7.1   | 192     | 99       | 0.53 | 4.71          | 0.147 $\pm$ 0.010                                      | 0.0227 $\pm$ 0.0009                                  | 144.7 $\pm$ 6.0                    |
| 8.1   | 1274    | 613      | 0.50 | 0.41          | 0.156 $\pm$ 0.006                                      | 0.0236 $\pm$ 0.0009                                  | 150.3 $\pm$ 5.9                    |
| 9.1   | 602     | 335      | 0.58 | 1.01          | 0.155 $\pm$ 0.006                                      | 0.0235 $\pm$ 0.0008                                  | 150.0 $\pm$ 5.6                    |
| S1.1  | 742     | 325      | 0.45 | 0.27          | 0.154 $\pm$ 0.006                                      | 0.0228 $\pm$ 0.0008                                  | 145.6 $\pm$ 5.4                    |
| S1.2  | 683     | 291      | 0.44 | 0.23          | 0.158 $\pm$ 0.006                                      | 0.0233 $\pm$ 0.0008                                  | 148.2 $\pm$ 5.5                    |
| S1.3  | 1678    | 723      | 0.45 | 0.37          | 0.156 $\pm$ 0.008                                      | 0.0241 $\pm$ 0.0008                                  | 153.2 $\pm$ 5.8                    |
| S1.4  | 359     | 112      | 0.32 | 0.67          | 0.152 $\pm$ 0.010                                      | 0.0233 $\pm$ 0.0008                                  | 148.7 $\pm$ 5.6                    |
| Weighted mean ( $2\sigma$ )                               |         |          |      |               |  |  |                                    |

with moderately variable  $^{147}\text{Sm}/^{144}\text{Nd}$  ratio (0.2845–0.4270). The fluorite sample S1 from the vein-type greisen is extremely enriched in Sm (125 ppm) and Nd (234 ppm) and relatively high in  $^{147}\text{Sm}/^{144}\text{Nd}$  ratio (0.3237). Among the analysed minerals, wolframite from the massive-type greisen exhibits the lowest Sm (1.2–1.6 ppm) and Nd (4.1–4.5 ppm) and least fractionated  $^{147}\text{Sm}/^{144}\text{Nd}$  ratio (0.1592–0.2333). On a conventional Sm–Nd isochron diagram (Fig. 3), all analysed minerals define a tightly linear isochron yielding an age of  $149 \pm 2$  Ma (MSWD = 0.102) and initial  $\epsilon\text{Nd}(T)$  values of  $-6.9 \pm 0.1$ .

## 6. Discussion and conclusions

New SHRIMP U–Pb zircon results indicate that the first and second phases of the Qianlishan granite,  $\gamma_5^{2a}$  and  $\gamma_5^{2b}$ , formed contemporaneously at  $152 \pm 2$  Ma, although the latter intruded the former (Wang *et al.* 1987; Mao *et al.* 1995). While this new U–Pb zircon age is indistinguishable within the analytical errors from the Rb–Sr isochron age of  $152 \pm 9$  Ma for  $\gamma_5^{2a}$  (Mao *et al.* 1995) and the muscovite K–Ar age of  $149.3 \pm 3.5$  Ma for  $\gamma_5^{2b}$  (Yin *et al.* 2002), it is more precise and accurate. Moreover, the  $\gamma_5^{2a}$  and  $\gamma_5^{2b}$  have

Table 2. Sm–Nd isotopic data for minerals from the Shizhuyuan polymetallic deposit, SE China

| Sample | Locality | Mineral    | Metasomatism         | Sm (ppm) | Nd (ppm) | $^{147}\text{Sm}/^{144}\text{Nd}$ | $^{143}\text{Nd}/^{144}\text{Nd} \pm 2\sigma_m$ |
|--------|----------|------------|----------------------|----------|----------|-----------------------------------|---|
| S4     | 490 m    | Garnet     | Massive-type skarn   | 3.00     | 2.31     | 0.7838                            | 0.512865 $\pm$ 0.000007                         |
| S14    | 490 m    | Garnet     | Massive-type skarn   | 6.26     | 11.8     | 0.3214                            | 0.512415 $\pm$ 0.000007                         |
| S14    | 490 m    | Fluorite   | Massive-type skarn   | 7.64     | 16.2     | 0.2845                            | 0.512380 $\pm$ 0.000005                         |
| KS4    | 380 m    | Wolframite | Massive-type skarn   | 15.9     | 22.5     | 0.4270                            | 0.512518 $\pm$ 0.000008                         |
| KS1    | 380 m    | Wolframite | Massive-type greisen | 1.20     | 4.54     | 0.1592                            | 0.512255 $\pm$ 0.000006                         |
| KS6    | 380 m    | Wolframite | Massive-type greisen | 1.59     | 4.11     | 0.2333                            | 0.512329 $\pm$ 0.000006                         |
| S1     | 490 m    | Fluorite   | Vein-type greisen    | 125      | 234      | 0.3237                            | 0.512417 $\pm$ 0.000007                         |

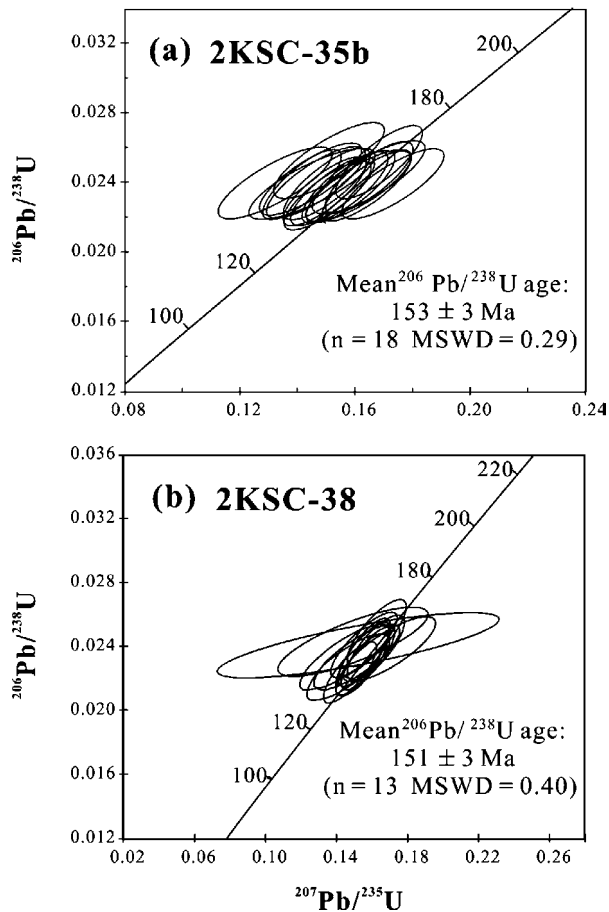


Figure 2. U–Pb concordia diagram showing analytical data for zircons from samples 2KSC35b (a) from the first phase ( $\gamma_5^{2a}$ ) and 2KSC38 (b) from the second phase ( $\gamma_5^{2b}$ ) of the Qianlishan granite.

nearly identical initial  $\epsilon\text{Nd}(T)$  values clustering around  $-6.4$  to  $-7.5$  (Mao, Li & Pei, 1995). Considering that the  $\gamma_5^{2a}$  and  $\gamma_5^{2b}$  comprise  $> 95\%$  of the exposed area of the Qianlishan pluton, these two major granite intrusions were co-genetic. It is noted that the  $\gamma_5^{2a}$  and  $\gamma_5^{2b}$  are highly fractionated granites having very high contents of Li, Be, Rb, Nb, Th, U and heavy rare earth elements (HREE) with REE patterns clearly showing the ‘tetrad effect’ (Shen *et al.* 1995; Mao *et al.* 1995; Zhao *et al.* 2001). Consequently, they have very high and variable  $^{87}\text{Rb}/^{86}\text{Sr}$  ratios of 24–318 and  $^{147}\text{Sm}/^{144}\text{Nd}$  ratios of 0.14–0.28. The older and younger Rb–Sr isochron dates reported previously (Wang *et al.* 1987; Shen *et al.* 1995; Mao, Li & Pei, 1995) are probably attributed to systematic analytical deviations of Rb/Sr. It is noteworthy that the granite porphyry ( $\gamma_5^{2d}$ ) has significantly lower  $^{87}\text{Rb}/^{86}\text{Sr}$  ratios of  $< 20$ ,  $^{147}\text{Sm}/^{144}\text{Nd}$  ratios of  $< 0.115$  and variable  $\epsilon\text{Nd}(T)$  values of  $-5.2$  to  $-8.6$ , indicating that the  $\gamma_5^{2d}$  might be independent of  $\gamma_5^{2a}$  and  $\gamma_5^{2b}$  in time and origin (Mao, Li & Pei, 1995).

Our mineral Sm–Nd age of  $149 \pm 2$  Ma is in good agreement within analytical error with the molybdenite

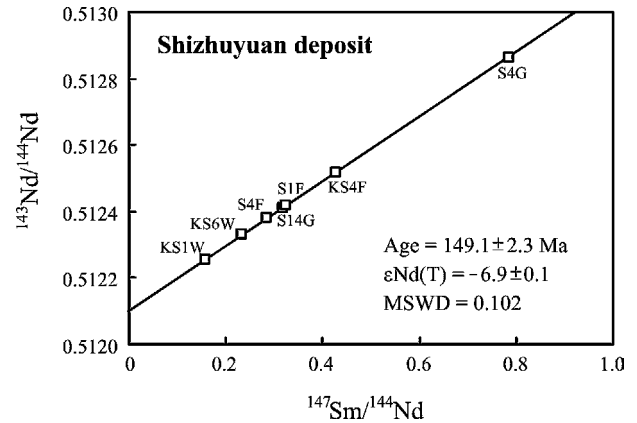


Figure 3. Sm–Nd isochron diagram for garnet, fluorite and wolframite mineral separates from skarn and greisen at the Shizhuyuan polymetallic deposit. Sm–Nd isochron age and  $\epsilon\text{Nd}(T)$  values were calculated using Isoplot/Ex 2.49 after Ludwig (2001), where 0.5% was chosen as the error of  $^{147}\text{Sm}/^{144}\text{Nd}$  ratios. Errors are quoted at the 95% confidence level. G – garnet; F – fluorite; W – wolframite.

Re–Os age of  $151 \pm 4$  Ma for the massive-type skarn-greisen (Li *et al.* 1996) and the muscovite K–Ar ages of  $148.0 \pm 2.9$  Ma for the vein-type greisen and  $146.5 \pm 2.9$  Ma for the massive-type greisen (Yin *et al.* 2002). Thus, the massive-type skarn-greisen and vein-type greisen were most likely coeval at  $149 \pm 2$  Ma. This age is just slightly younger than, or strictly speaking, indistinguishable within error from the granite age of  $152 \pm 2$  Ma, indicating that the supergiant W–Sn–Mo–Bi mineralization at the Shizhuyuan formed contemporaneously with, or very shortly after, the intrusion of the Qianlishan granite plutonism. Therefore, the time interval between the plutonism and the mineralization is likely  $< 2$  Myr. The minerals from skarn and greisen have quite uniform  $\epsilon\text{Nd}(T)$  values of  $-6.9$ , identical to those of the  $\gamma_5^{2a}$  and  $\gamma_5^{2b}$  ( $\epsilon\text{Nd}(T) = -6.4$  to  $-7.5$ ; Mao *et al.* 1995), suggesting a derivation of REE in metasomatic fluids from the host granite.

In addition to the Shizhuyuan deposit and Qianlishan granite, many other important non-ferrous and rare metal deposits are also related to some small, highly fractionated granite plutons and stocks within the Early Yanshanian granitoid province. These deposits include the greisen-skarn type W–Sn–Bi–Mo–Be deposit at Yaogangxian, the hypothermal vein-type wolframite deposit at Xihuashan, the albitization granite type W–Nb–Ta–REE deposit at Dajishan and the alteration granite-skarn-hydrothermal replacement-type Nb–Ta–W–Sn–Be–Pb–Zn deposit at Xianghualing (Pei & Hong, 1995). Although on a regional scale the most significant granitic activity occurred from 164–153 Ma (Li, 2000), the precise timing of the emplacement of the highly fractionated plutons and generation of their related non-ferrous and rare metal mineralization awaits further high-precision geochronology investigations.

**Acknowledgements.** We thank Y. M. Liu and Y. Z. Xu for assistance in field works. Review comments from two anonymous reviewers significantly improved the manuscript. This work was supported by the Ministry of Science and Technology of China (grants G1999043201), Chinese Academy of Sciences (grant KZCX2-101) and NSFC (grant 49725309).

## References

- BLICHERT-TOFT, J. & FREI, R. 2001. Complex Sm–Nd and Lu–Hf isotope systematics in metamorphic garnets from the Isua supracrustal belt, West Greenland. *Geochimica et Cosmochimica Acta* **65**, 3177–87.
- BLACK, L. P., KAMO, S. L., ALLEN, C. M., ALEINIKOFF, J. N., DAVIS, D. W., KORSCH, R. J. & FOUDOULIS, C. 2003a. TEMORA 1: a new zircon standard for Phanerozoic U–Pb geochronology. *Chemical Geology* **200**, 155–70.
- BLACK, L. P., KAMO, I. S., WILLIAMS, C. M., MUNDIL, R., DAVIS, D. W., KORSCH, R. J. & FOUDOULIS, C. 2003b. The application of SHRIMP to Phanerozoic geochronology: a critical appraisal of four zircon standards. *Chemical Geology* **200**, 171–88.
- CUMMING, G. L. & RICHARDS, J. R. 1975. Ore lead isotope ratios in a continuously changing Earth. *Earth and Planetary Science Letters* **28**, 155–71.
- LAZNICKA, P. 1999. Quantitative relationships among giant deposits of metals. *Economic Geology* **94**, 455–74.
- LI, H. Y., MAO, J. W., SUN, Y. L., ZOU, X. Q., HE, H. L. & DU, A. D. 1996. Re–Os isotopic chronology of the molybdenites in the Shizhuyuan polymetallic tungsten deposit, southern Hunan. *Geological Review* **42**, 261–7 [in Chinese with English abstract].
- LI, X. H. 2000. Cretaceous magmatism and lithospheric extension in Southeast China. *Journal of Asian Earth Sciences* **18**, 293–305.
- LIANG, X. R., WEI, G. J., LI, X. H. & LIU, Y. 2003. Precise determination of  $^{143}\text{Nd}/^{144}\text{Nd}$  and Sm/Nd ratios using multiple-collector inductively coupled plasma-mass spectrometer (MC-ICPMS). *Geochimica* **32**, 91–6 [in Chinese with English abstract].
- LIU, Y. J., ZHANG, J. R. & CHEN, J. 1983. Study on some problems about metallogenesis of the Shizhuyuan tungsten, molybdenum, bismuth, tin (beryllium) deposit. *Geology and Exploration* **19**, 8–14 [in Chinese].
- LIU, Y. M., DAI, T. M., LU, H. Z., XU, Y., WANG, C. L. & KANG, W. Q. 1997.  $^{40}\text{Ar}$ – $^{39}\text{Ar}$  and Sm–Nd isotopic ages for the Qianlishan granite and its mineralization. *Science in China (Series D)* **27**, 425–30 [in Chinese].
- LUDWIG, K. 2001. *Isoplot/Ex 2.49. A Geochronological Toolkit for Microsoft Excel*. Berkeley Geochronology Center, Berkeley, CA, USA, Special Publication no. 1a.
- MAO, J. W., LI, H. Y. & PEI, R. 1995. Nd–Sr isotopic and petrogenetic studies of the Qianlishan granite stock, Hunan Province. *Mineral Deposits* **14**, 235–42 [in Chinese with English abstract].
- MAO, J. W., LI, H. Y., PEI, R., RAIMBAULL, L. & GUY, B. 1995. Geology and geochemistry of the Qianlishan granite stock and its relationship to polymetallic tungsten mineralization. *Mineral Deposits* **14**, 12–25 [in Chinese with English abstract].
- MAO, J. W., GUY, B., RAIMBAULL, L. & SHIMAZAKI, H. 1996. Manganese skarn in the Shizhuyuan polymetallic tungsten deposit, Hunan, China. *Resource Geology* **46**, 1–11.
- MAO, J. W., LI, H. Y., SONG, X. X., RUI, B., XU, Y., WANG, D. H., LAN, X. M. & ZHANG, K. J. 1998. *Geology and Geochemistry of the Shizhuyuan W–Sn–Mo–Bi Polymetallic Deposit, Hunan, China*. Beijing: Geological Publishing House, 215 pp.
- PEI, R. & HONG, D. 1995. The granites of South China and their metallogeny. *Episodes* **18**, 77–82.
- SHEN, W., WANG, D., XIE, Y. & LIU, C. 1995. Geochemical characteristics and Material sources of the Qianlishan composite granite body, Hunan Province. *Acta Petrologica et Mineralogica* **14**, 193–202 [in Chinese with English abstract].
- SONG, B., ZHANG, Y., WAN, Y. & JIAN, P. 2002. Mount making and procedure of the SHRIMP dating. *Geological Review* **48**(suppl.), 26–30 [in Chinese with English abstract].
- TANAKA, T. & 19 co-authors. 2000. JNdi-1: a neodymium isotopic reference in consistency with LaJolla neodymium. *Chemical Geology* **168**, 279–81.
- THÖNI, M. 2002. Sm–Nd isotope systematics in garnet from different lithologies (Eastern Alps): age results, and an evaluation of potential problems for garnet Sm–Nd chronometry. *Chemical Geology* **185**, 255–81.
- VANCE, D. & THIRLWALL, M. 2002. An assessment of mass discrimination in MC-ICPMS using Nd isotopes. *Chemical Geology* **185**, 227–40.
- WANG, C. L., LUO, S., XU, Y., SUN, Y., XIE, C., ZHANG, Z., XU, W. & REN, X. 1987. *Geology of the Shizhuyuan Tungsten-Polymetallic Deposit*. Beijing: Geological Publishing House, 173 pp.
- WILLIAMS, I. S. 1998. U–Th–Pb geochronology by ion microprobe. In *Applications of microanalytical techniques to understanding mineralizing processes* (eds M. A. McKibben, W. C. Shanks and W. I. Ridley), pp. 1–35. *Review of Economic Geology* **7**.
- YIN J., KIM, S. J., LEE, H. K. & ITAYA, T. 2002. K–Ar ages of plutonism and mineralization at the Shizhuyuan W–Sn–Bi–Mo deposit, Hunan Province, China. *Journal of Asian Earth Sciences* **20**, 151–55.
- ZHAO, Z. H., BAO, Z. W., ZHANG, B. Y. & XIONG, X. L. 2001. Crust-mantle interaction and its contribution to the Shizhuyuan superlarge tungsten polymetallic mineralization. *Science in China (Series D)* **44**, 266–76.